



# Magnetic field variations and a giant flare

## Multiwavelength observations of CN Leo

C. Liefke<sup>1</sup>, A. Reiners<sup>1,2</sup>, and J. H. M. M. Schmitt<sup>1</sup>

<sup>1</sup> Hamburger Sternwarte, Gojenbergsweg 112, D-21029 Hamburg, Germany; e-mail: [cliefke@hs.uni-hamburg.de](mailto:cliefke@hs.uni-hamburg.de)

<sup>2</sup> Georg-August-Universität Göttingen, Institut für Astrophysik, Friedrich-Hund-Platz 1, D-37077 Göttingen, Germany

**Abstract.** The M5.5 dwarf CN Leo has been observed simultaneously with *XMM-Newton* and VLT/UVES on three nights in May 2006. Nightly variations of its magnetic field are deduced from FeH lines in the UVES spectra. A giant flare occurred and is covered in total by all instruments. Time-resolved spectroscopy in X-rays traces the development of temperature and emission measure of the coronal flaring plasma. Coronal densities  $\log n_e > 12$  are derived during the flare from the O VII triplet. The UVES spectra simultaneously trace the behavior of chromospheric and transition region plasmas. Large increases in the fluxes of chromospheric emission lines are accompanied by a strong enhancement of the continuum level. The Balmer lines show strong broadening and lines of the hydrogen Paschen series are observed in emission during the flare.

**Key words.** Stars: activity – Stars: magnetic fields – Stars: flare – Stars: coronae – Stars: individual: CN Leo – X-rays: stars

### 1. Introduction

In active M dwarfs stellar activity indicators like chromospheric H $\alpha$  emission and coronal X-ray emission can reach values orders of magnitude higher than observed in the Sun. Substantial variability can be seen in all wavelength bands, and frequent and strong flaring with flux increases by factors up to several hundreds is widespread among these objects (e. g. Güdel et al. 2002; Stelzer et al. 2006). The origin of these flare events is usually ascribed to magnetic reconnection, with the underlying magnetic fields of active M dwarfs reaching up

to several kG with large surface filling factors (Johns-Krull & Valenti 1996). We investigate the correlated time variability of photospheric magnetic fields with chromospheric and coronal activity indicators on the active M dwarf CN Leo in a time series that includes a giant flare.

### 2. Observations

Simultaneous observations of CN Leo have been performed with *XMM-Newton* and the UVES spectrograph at the VLT during three nights in May 2006. High time resolution photometry is provided by *XMM*'s EPIC instruments in X-rays and by its Optical Monitor

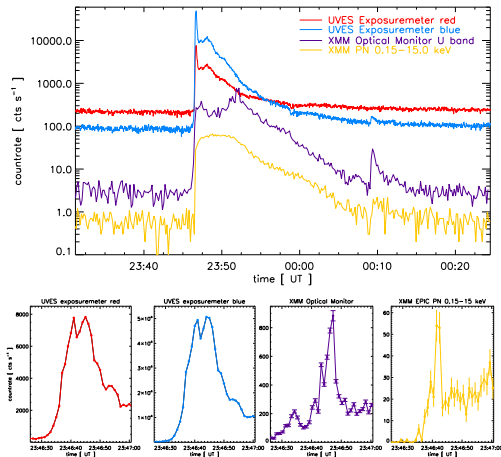


**Fig. 1.** Top: Lightcurves of the giant flare in different spectral bands. Bottom: the impulsive phase of the flare.

(OM) in the U band, and by the two UVES exposuremeters (blue and red). The UVES spectrograph was operated in dichroic mode with spectral coverage from 3200 Å to 3860 Å in the UV and in the red band from 6400 Å to 10080 Å with a gap between 8190 Å and 8400 Å. UVES exposure times varied according to seeing conditions from 100 s to 300 s in the red arm and from 1000 s to 1500 s in the blue arm, resulting in 68, 24 and 89 red spectra, and in 16, 5 and 11 blue spectra in the three nights, respectively.

### 3. The giant flare

A huge flare with flux increases by factors up to 500 in the optical and up to 100 in X-rays occurred on 19 May at 23:47 UT and lasted for approximately 25 minutes. Lightcurves in different spectral bands are shown in Fig. 1. A strong impulsive outburst is followed by a second peak in the optical, while in X-rays the count rate stays constant for about five minutes. The decrease in count rate in the red and blue optical bands is initially very fast and then slows down, while the decay rate seems to be constant in X-rays and in the U band. Note that the EPIC instruments are affected by pile-up (up to 30% during the flare peak) and the

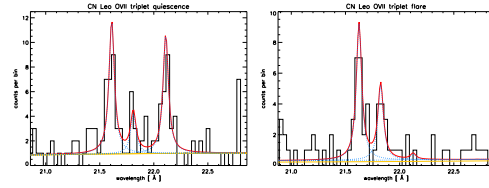


**Fig. 2.** O VII triplet in RGS1, extracted from the quiescent part of the first X-ray observation (exposure time 20.8 ks, left) and covering the giant flare (1.4 ks, right).

OM lightcurve is corrupted by disproportionate dead-time and coincidence loss corrections for count rates higher than  $\approx 500$  cts s $^{-1}$ . The first 30 seconds of the flare (Fig. 1, bottom) cover the impulsive outburst. The optical bands behave very similar apart from the different amplitude, while the U band lightcurve shows a precursing event followed by the main outburst. A very short outburst is visible in X-rays, the adjacent rise to the peak count rate is outside the plotting range.

X-ray spectra covering the initial rise phase, the “plateau” of constant count rate at the flare peak, and the decay phase of the giant flare clearly demonstrate the development of the coronal plasma during the flare. Compared to quiescence, a strong increase in temperature and emission measure sets in with the flare rise. Enhanced line emission between 0.6 and 1.1 keV sets in at the peak, while during the decay phase the emission measure slowly decreases with temperatures still at high levels. Coronal densities can be inferred from the flux ratio of the forbidden and intercombination lines of He-like O VII (Fig. 2). In quiescence, the  $f/i$  ratio is  $2.88 \pm 1.53$ , indicating  $\log n_e \approx 10$  but within the errors still consistent with the low-density limit, while during the flare the density increases to  $\log n_e > 12$ , as determined by  $f/i = 0.08 \pm 0.15$ .

The UVES spectra show a strong continuum enhancement during the flare. While continuum emission in the blue part of the spectra is almost absent outside the flare, a strong enhancement is visible during the rise phase. Strong chromospheric line emission and broadening of the Balmer lines does not set in until the flare peak is reached. In the red part of

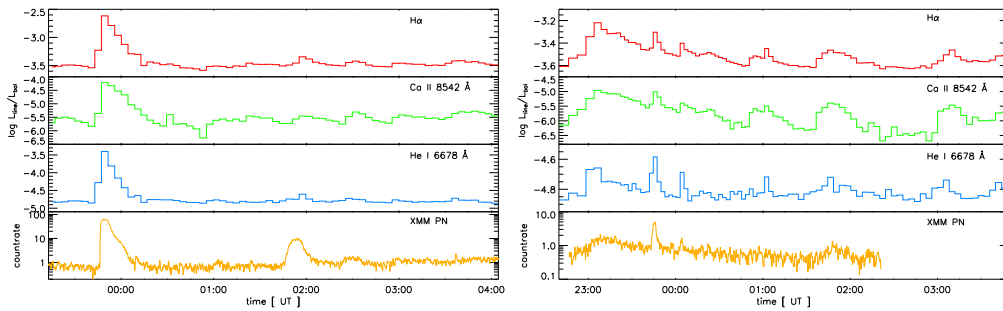


**Fig. 3.** Temporally resolved behavior of H $\alpha$ , Ca II at 8542 Å, He I at 6678 Å and X-ray flux during the two nights of 19/20 May (left) and 23/24 May (right).

the spectra Ca II at 8498 Å, 8542 Å and 8662 Å as well as He I at 6678 Å and 7065 Å are clearly in emission during the flare. The broad absorption lines of K I and Na I develop emission line cores or are filled up. A disproportionately higher flux is visible during the flare around 10049 Å at the wavelength position of Paschen  $\delta$ . Assuming that the flare covers only a small part of the stellar surface, we subtracted the quiescent spectrum from the flare spectra to obtain the pure flare emission. In these spectra lines of the Paschen series from Paschen  $\delta$  to Paschen 10 are clearly observed in emission, indicating extremely high densities in the lower chromosphere according to Houdebine & Doyle (1994), while the Balmer lines trace the upper chromosphere.

Fig. 3 shows the development of chromospheric emission line fluxes compared to the X-ray flux during two of the three nights, covering especially the huge flare. The lines are good tracers of the X-ray lightcurve also for smaller variations. Note the different cooling timescales for the giant flare.

#### 4. Magnetic fields

Reiners & Basri (2006) introduced a method to measure the mean photospheric magnetic flux (field strength  $\times$  filling factor,  $Bf$ ) for very late type stars from lines of the FeH absorption band around 9950 Å. We determined the magnetic flux of CN Leo from each of the red UVES spectra. The average magnetic flux varies by  $\approx 100$  G from 1<sup>st</sup> to 2<sup>nd</sup> night and by  $\approx 25$  G from 2<sup>nd</sup> to 3<sup>rd</sup> night, see Fig. 4. The

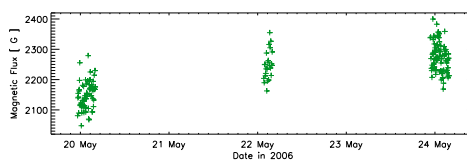


**Fig. 4.** Measured magnetic flux of CN Leo in the three nights.

scatter of the data points for each night suggests additional intra-night variability. Also, a slight increase of magnetic field strength is observed before the flare, indicating a compression of the field lines, and after the reconnection event the magnetic flux drops. However, its significance is not clear since other variations in the magnetic flux lightcurve are of the same amplitude and it is difficult to distinguish them from the measurement uncertainties.

#### References

- Güdel, M., Audard, M., Skinner, S. L., & Horvath, M. I. 2002, *ApJ*, 580, L73
- Houdebine, E. R. & Doyle, J. G. 1994, *A&A*, 289, 185
- Johns-Krull, C. M. & Valenti, J. A. 1996, *ApJ*, 459, L95
- Reiners, A. & Basri, G. 2006, *ApJ*, 644, 497
- Stelzer, B., Schmitt, J. H. M. M., Micela, G., & Liefke, C. 2006, *A&A*, 460, L35